Bulgarian Journal of Physics **28** Nos 3/4 (2001) 168-174

ELECTRICAL AND MAGNETIC PROPERTIES OF $(Pb_{0.7}Sn_{0.3})Sr_2(Y_{0.6}Ca_{0.4})Cu_2O_z$

N. BALCHEV
Institute of Solid State Physics, Bulgarian Academy of Sciences
72 Tzarigradsko Chaussée Blvd, 1784 Sofia, Bulgaria

K. NENKOV, J. WARCHULSKA, Y. SKOURSKI,
V. NIZHANKOVSKII
Int. Laboratory of High Magnetic Fields and Low Temperatures
53-421 Wroclaw, Poland

B. KUNEV
Institute of Catalysis, Bulgarian Academy of Sciences
1113 Sofia, Bulgaria

A. SOULEVA
University of Chemical Technology and Metallurgy
1756 Sofia, Bulgaria

TS. TSACHEVA
Institute of Physical Chemistry, Bulgarian Academy of Sciences
1113 Sofia, Bulgaria

Abstract. The effect of Sn-doping in $(Pb,Cu)Sr_2(Y_{0.6}Ca_{0.4})Cu_2O_z$ was investigated. The results of the XRD, ICP-AES and EDX on SEM analyses showed that the obtained material contained the phase 1212. The EDX analysis in different points showed that tin was present in most of the microcrystals but its distribution was inhomogeneous. The resistivity and susceptibility measurements denoted superconductivity at $T_c = 20$ K. The dependence of the resistance on the magnetic field showed about 20 % of magnetoresistance effect at 4.2 K, which coexisted with the superconducting state up to $H = 1$ kŒ. The low values of T_c and the magnetoresistance were explained by assuming that a part of Sn occupied copper positions in the CuO_2 planes.

PACS number: 74.25.Ha

1. Introduction

After the discovery of the nonsuperconducting lead-based 1212 cuprate $(Pb,Cu)Sr_2(Y,Ca)Cu_2O_7$ [1] many attempts have been made to induce or optimize the superconductivity in this material. They included the optimization of synthesis conditions and Y/Ca ratio as well as various chemical substitutions. As a result superconductors with transition temperatures T_c from 17 K [2] to 105 K [3] were obtained. Lee and Han [4] summarized that the cationic sizes of the substituting elements varied from 0.72 Å for Mg to 1.18 Å for Sr. To our knowledge the tin substitution in the (Pb,Cu)-1212 material has not been investigated. It was established that Sn stimulated the Hg-1212 phase formation [5] and even could form a tin-based 1212 structure [6].

The purpose of the present work is to investigate the effect of the Sn doping (cationic radius 0.69 Å) on the superconducting properties of $(Pb,Cu)Sr_2(Y_{0.6}Ca_{0.4})Cu_2O_z$ as well as to study the magnetoresistance of the obtained material.

2. Results and Discussion

The investigated samples with nominal composition $(Pb_{0.7}Sn_{0.3})Sr_2(Y_{0.6}Ca_{0.4})$-$Cu_2O_z$ as well as those with different Sn content were prepared by a solid state reaction in air from starting materials PbO, SnO_2, $SrCO_3$, Y_2O_3, $CaCO_3$ and CuO with a purity of 99.9 %. Here we used the difference in the valence states of Pb(II) and Sn(IV) in order to stabilize the phase 1212 [7]. They were mixed, homogenized, pressed into pellets and fired at 800–840 °C for 20 h. The resulting material was reground and pressed into pellets. The latter were sintered at 850–950 °C for 30–120 hours and quenched to room temperature. X-ray diffraction (XRD) was used to examine the samples using a TUR-M62 diffractometer. An inductively coupled plasma atomic emission spectrometry (ICP-AES) was performed to powdered samples by using an ICP spectrometer "Plasma 40" of Perkin-Elmer. An EDX on SEM analysis was also performed on the pellets using a Jeol Superprobe 733 microscope. The resistance of the samples vs temperature $R(T)$ was measured by using the standard four probe method. The susceptibility of the samples was measured as a function of temperature $\chi(T)$ using a Faraday type susceptometer (Cahn balance), as well as a Lake Shore 7000 Series AC susceptometer–DC magnetometer at a frequency of 133 Hz. The resistance of the samples vs the magnetic field was measured by using a superconducting magnet in the range of 0.2–120 kŒ.

Figure 1 shows the XRD patterns of samples with different Sn content. It may be seen in the figure that all the samples contain a dominating 1212 phase. The undoped $(Pb_{0.6}Cu_{0.4})Sr_2(Y_{0.6}Ca_{0.4})Cu_2O_z$ is multiphase (curve *a*) and this is in agreement with the results of Ono and Uchida [2]. The doped

$(Pb_{0.6}Sn_{0.1}Cu_{0.3})Sr_2(Y_{0.6}Ca_{0.4})Cu_2O_z$ has an improved phase purity (curve *c*). The samples *a*–*c* contain a $SrCu_2O_3$ impurity. The curve *d* shows the XRD pattern of a $(Pb_{0.7}Sn_{0.3})Sr_2(Y_{0.6}Ca_{0.4})Cu_2O_z$ sample, syntesized at 900 °C. This composition is also multiphase but contains a $SrSnO_3$ as impurity. The calculated lattice parameters are $a = 3.805$ Å and $c = 11.780$ Å.

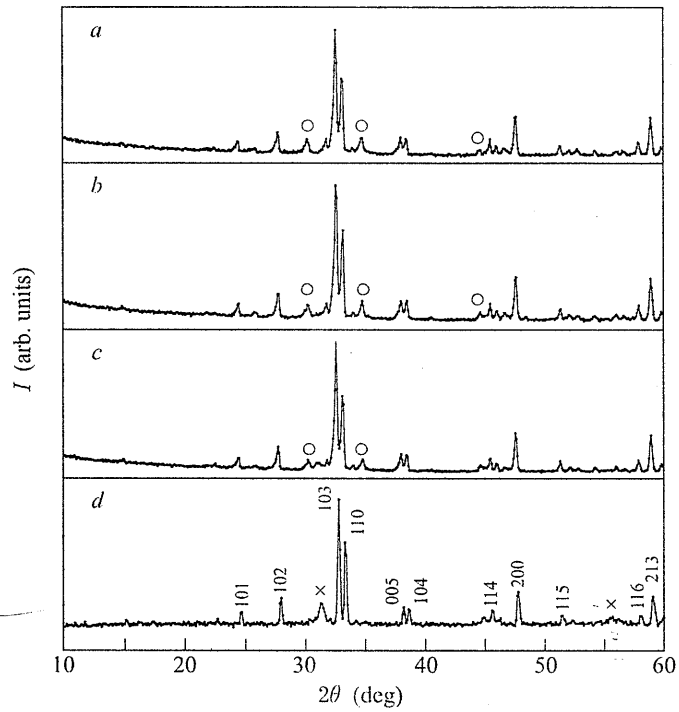

Fig. 1. XRD patterns of samples with different Sn content (*a*) $(Pb_{0.6}Cu_{0.4})Sr_2(Y_{0.6}Ca_{0.4})Cu_2O_z$; (*b*) $(Pb_{0.6}Sn_{0.05}Cu_{0.35})Sr_2(Y_{0.6}Ca_{0.4})Cu_2O_z$; (*c*) $(Pb_{0.6}Sn_{0.1}Cu_{0.3})Sr_2(Y_{0.6}Ca_{0.4})Cu_2O_z$; (*d*) $(Pb_{0.7}Sn_{0.3})Sr_2(Y_{0.6}Ca_{0.4})Cu_2O_z$. ○ — $SrCu_2O_3$ and × — $SrSnO_3$

In order to obtain the quantities of the different elements, an ICP-AES analysis is performed to the $(Pb_{0.7}Sn_{0.3})Sr_2(Y_{0.6}Ca_{0.4})Cu_2O_z$ sample. If it is assumed that Sr^{2+} sites are occupied solely by these ions, and that the overall occupancy of the (Y,Ca) sites must be unity, a chemical composition of $(Pb_{0.5}Sn_{0.32}Ca_{0.12})Sr_2(Y_{0.62}Ca_{0.38})Cu_{2.03}O_z$ should be obtained. A significant loss of Pb was observed at higher synthesis temperatures and this effect should be discussed later.

In order to check for the presence of Sn in the individual microcrystals, an EDX on SEM analysis was performed on the same sample. The results of this

analysis on 10 different points are given in Table 1. It may be seen in the table that all the investigated points have a composition, close to 1212. The Sn content varies from 0.3 for point 1 to 0.05 for point 7. This result shows that tin enters most of the microcrystals but its distribution is inhomogeneous. The points 9 and 10 contain only Ca-doped (Pb,Cu)-1212 phase. Rouillon et al [8] have shown that the Ca substitution is favourable to the (Pb,Cu)-1212 superconductor and Deng et al [9] that Ca for Y substitution could be an useful method to adjust carrier concentration in many superconductors.

Table 1. Chemical compositions in different points of the $(Pb_{0.7}Sn_{0.3})Sr_2(Y_{0.6}Ca_{0.4})$-$Cu_2O_z$ sample, according to the EDX on SEM analysis

Point	Composition
1	$(Pb_{0.5}Sn_{0.3}Ca_{0.04}Cu_{0.02})Sr_2(Y_{0.7}Ca_{0.3})Cu_2O_z$
2	$(Pb_{0.48}Sn_{0.18}Ca_{0.05})Sr_2(Y_{0.76}Ca_{0.24})Cu_2O_z$
3	$(Pb_{0.55}Sn_{0.11}Ca_{0.19}Cu_{0.15})Sr_2(Y_{0.75}Ca_{0.25})Cu_{2.2}O_z$
4	$(Pb_{0.55}Sn_{0.1}Ca_{0.17}Cu_{0.18})Sr_2(Y_{0.78}Ca_{0.22})Cu_{2.27}O_z$
5	$(Pb_{0.54}Sn_{0.09}Ca_{0.09}Cu_{0.28})Sr_2(Y_{0.73}Ca_{0.27})Cu_{2.05}O_z$
6	$(Pb_{0.5}Sn_{0.11}Ca_{0.12}Cu_{0.27})Sr_2(Y_{0.8}Ca_{0.2})Cu_{2.01}O_z$
7	$(Pb_{0.55}Sn_{0.05}Ca_{0.11}Cu_{0.25})Sr_2(Y_{0.76}Ca_{0.24})Cu_2O_z$
8	$(Pb_{0.55}Sn_{0.06}Ca_{0.12}Cu_{0.27})Sr_2(Y_{0.76}Ca_{0.24})Cu_2O_z$
9	$(Pb_{0.68}Ca_{0.1}Cu_{0.22})Sr_2(Y_{0.65}Ca_{0.35})Cu_{2.68}O_z$
10	$(Pb_{0.55}Ca_{0.16}Cu_{0.11})Sr_2(Y_{0.8}Ca_{0.2})Cu_2O_z$

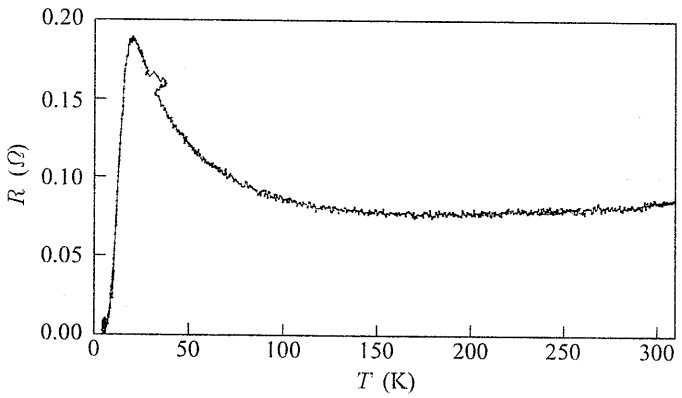

Fig. 2. $R(T)$ dependency of a $(Pb_{0.7}Sn_{0.3})Sr_2(Y_{0.6}Ca_{0.4})Cu_2O_z$ sample, synthesized at 935 °C

The susceptibility measurements have shown that the samples a–c of Fig. 1 are not superconducting down to 4.2 K. Figure 2 shows the $R(T)$ dependency of $(Pb_{0.7}Sn_{0.3})Sr_2(Y_{0.6}Ca_{0.4})Cu_2O_z$, synthesized at 935 °C. It may be seen in the figure the presence of a semiconducting behaviour in the normal state and

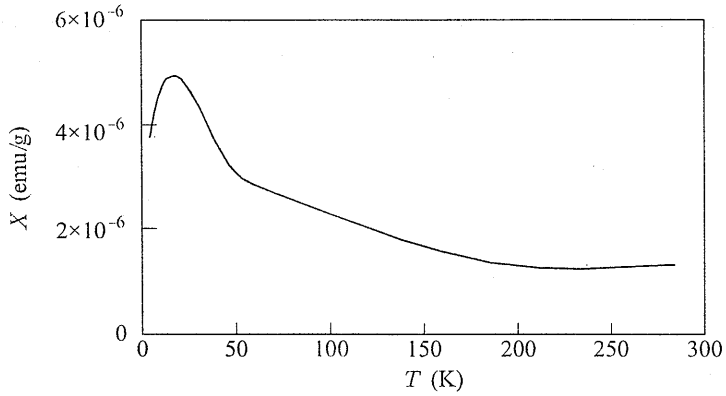

Fig. 3. $\chi(T)$ dependency of the same sample, measured by Cahn balance

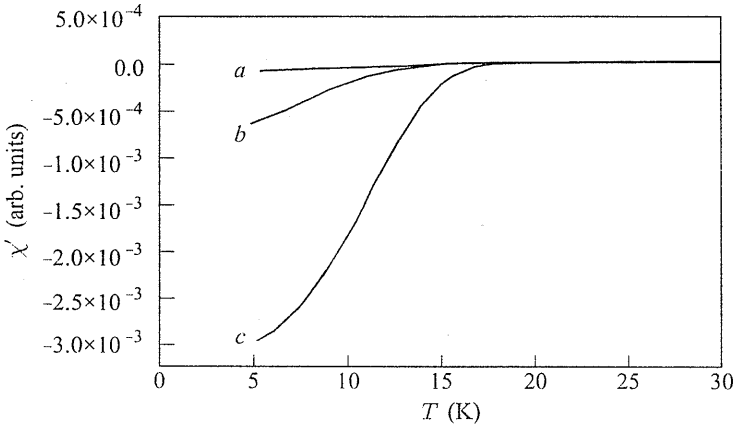

Fig. 4. Dependences of χ on T for $(Pb_{0.7}Sn_{0.3})Sr_2(Y_{0.6}Ca_{0.4})Cu_2O_z$ sample measured with AC susceptometer
Sample synthesized at different temperatures: (*a*) 900 °C; (*b*) 920 °C and (*c*) 935 °C

a transition at $T_{on} = 20$ K. The $R(T)$ dependency, measured in the residual field of $H = 100$ Œ of the superconducting magnet show a $T_{on} = 15$ K and a transition is not found at $H = 50$ kŒ. In Fig. 3 the dependence of $\chi(T)$ for the same sample, measured with a Faraday type susceptometer (Cahn balance) is given. The measurement is done at a field of $H = 0.5$ kŒ. It may be seen in the figure the presence of a diamagnetic transition at $T_c = 20$ K, which value corresponds with that of the resistive transition. Figure 4 shows the susceptibility curves for samples, synthesized at different temperatures measured by AC susceptometer at $H = 0$. It may be seen in the figure that the T_c increases from 12 K for the sample, prepared at 900 °C (curve *a*) to 17 K for that synthesized at 935 °C (curve *c*). This is accompanied with an increase

of the superconducting volume fraction. At $H = 1$ kŒ the superconductivity still exists, but T_c is reduced to 8 K. Superconductivity is not observed if the synthesis temperature is higher than 940 °C. This is attributed to the increase of Pb loss at higher temperatures. For example a sample, synthesized at 945 °C has a chemical composition of $(Pb_{0.22}Sn_{0.32}Ca_{0.15}Cu_{0.1})Sr_2(Y_{0.65}Ca_{0.35})Cu_2O_z$, according to the ICP-AES analysis. Also the lattice parameters of this non-superconducting sample slightly increase in comparison with those of the superconducting one, synthesized at 900 °C: $a = 3.810$ Å and $c = 11.786$ Å, as in [2]. The strong Pb deficiency is compensated by an increase of oxygen atoms in the rocksalt layers. Oxygen in this position tends to trap holes within the rocksalt layer and thus limits the T_c of the unsubstituted (Pb,Cu)-1212 system to 45-67 K [10]. A further reduction of T_c could occur if some Sn occupies copper positions in the CuO_2 planes.

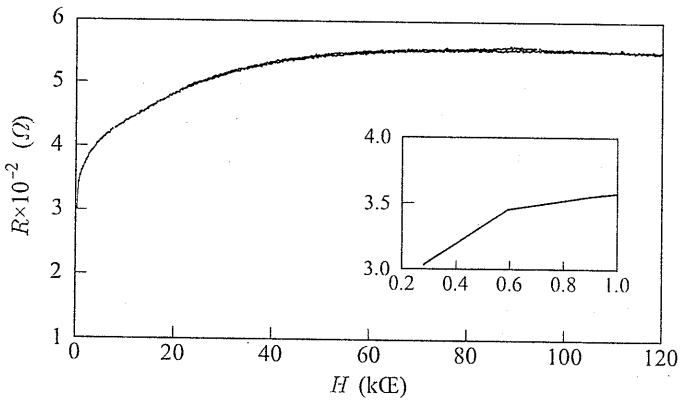

Fig. 5. Dependence of the resistance R on the magnetic field H at 4.2 K for a $(Pb_{0.7}Sn_{0.3})Sr_2(Y_{0.6}Ca_{0.4})Cu_2O_z$ sample
Sample synthesized at 935 °C. Inset: extended scale in the region 0.2-1 kŒ

Figure 5 shows the dependence of the resistance on the magnetic field for the sample, synthesized at 935 °C. The measurement is done at 4.2 K. It may be seen in the figure the presence of about 60 % of magnetoresistance effect at $H = 120$ kŒ. The inset is an extended scale in the region 0.2-1 kŒ, where the superconductivity exists. A change in the slope of the curve at $H = 0.6$ kŒ may be seen in the figure and a magnetoresistance effect of about 20 % at $H = 1$ kŒ, which coexists with the superconducting state. The magnetoresistance could be explained if we assume that a part of Sn occupies some Cu positions in the CuO_2 planes. In this case it will act as a magnetic impurity according to the Hubbard model, as stated in [11]. However the contribution of the Sn-containing impurity cannot be excluded.

3. Conclusion

The effect of Sn-doping in (Pb,Cu)$Sr_2(Y_{0.6}Ca_{0.4})Cu_2O_z$ was investigated. The results of the XRD, ICP-AES and EDX on SEM analyses showed that the obtained material contained the phase 1212. The EDX analysis in different points showed that Sn was present in most of the microcrystals. The resistivity and susceptibility measurements showed that the material was superconducting at $T_c = 20$ K. The investigation of the magnetoresistance showed the presence of about 20 % magnetoresistance effect at 4.2 K, which coexisted with the superconducting state up to $H = 1$ kŒ. The low values of T_c and the magnetoresistance of the obtained material were attributed to the partial occupancy of the tin of copper positions in the CuO_2 planes.

Attempts to increase the critical temperature and superconducting volume fraction of the samples are in progress.

Acknowledgments

The authors gratefully acknowledge Prof. Dr V. Kovachev from the Institute of Solid State Physics for the helpful discussions, as well as Assoc. Prof. Dr I. Nedkov from the Institute of Electronics for his contribution in the synthesis of the samples.

References

1. M. Subramanian, J. Gopalakrishnan, C. Torardi, P. Gai, E. Boyes, T. Askew, R. Flippen, W. Farneth and A. Sleith. Physica C **159** (1989) 124.
2. A. Ono and Y. Uchida. Jap. J. Appl. Phys. **29** (1990) L586.
3. R. Liu, P. Edwards, Y. Huang, S. Wu and P. Wu. J. Solid State Chem. **86** (1990) 334.
4. H. Lee and G. Han. Supercond. Sci. Technol. **12** (1999) 177.
5. N. Balchev, F. Van Allemeersch, F. Persyn, J. Schroeder, R. Deltour and S. Hoste. Supercond. Sci. Technol. **10** (1997) 65.
6. Y. Yu, X. Xu, X. Jin, S. Ding, Z. Zheng, X. Yao and G. Shen. Phys. Stat. Sol. (a) **163** (1997) 177.
7. B. Raveau, C. Michel, M. Hervieu, G. Van Tendeloo. A. Maignan, Ann. Chim. Fr. **19** (1994) 487.
8. T. Rouillon, A. Maignan, M. Hervieu, C. Michel, D. Groult and B. Raveau. Physica C **171** (1990) 7.
9. H. Deng, C. Dong, Y. Zhou, F. Wu, H. Chen, S. Jia, J. Shen, G. Yuan, Z. Zhao. Physica C **296** (1998) 225.
10. M. Kosuge, T. Maeda, K. Sakuyama, H. Yamauchi, N. Koshizuka and S. Tanaka. Physica C **182** (1991) 157.
11. Y. Zhao, B. Chen, H. Kennedy, H. Zhang, F. Wang. Physica C **252** (1995) 381.

Bulgarian Journal of Physics **28** Nos 3/4 (2001) 175-184

VARIABLE STARS IN THE OUTER-HALO GLOBULAR CLUSTER PALOMAR 3

J. BORISSOVA, N. SPASSOVA
Institute of Astronomy, Bulgarian Academy of Sciences
72 Tzarigradsko Chaussée Blvd, 1784 Sofia, Bulgaria

V. IVANOV
Steward Observatory, University of Arizona
Tucson, AZ 85721, USA

Abstract. We present the time-series V and I photometry of the outer-halo globular cluster Palomar 3, which has been obtained with a purpose of providing the extensive CCD variability study of this cluster. As a result, we have confirmed the variability of the RR Lyr star candidate of Burbidge and Sandage (1958), the RR Lyr star suspected by Gratton and Ortolani (1984) and the Population II Cepheid. Seven new suspected variables are presented. For the first time we determine the period $P = 3.402$ days and the light curve of the Population II Cepheid. As well known, Population II Cepheids are usually found in clusters with well-developed blue-HB tails only, so their presence in such a red-HB cluster as Palomar 3 is extremely puzzling.

PACS number: 97.30.-b

1. Introduction

Obtaining complete samples of RR Lyr variables in Galactic globular clusters is a very important observational task. The pulsation characteristics of these variables reflect the values assumed by their underlying physical parameters (mass, luminosity, temperature, chemical composition), and thus provide a sensitive tool to analyze the physical properties of horizontal-branch (HB) stars. Moreover, knowledge of the "real" number of RR Lyr variables in a globular cluster is required for the computation of the HB morphology parameters, such as $(B-R)/(B+V+R)$, which are usually employed in the analysis of the second-parameter problem.

Palomar 3 is an outer-halo $R_{GC} \simeq 89.9$ kpc, metal-intermediate [Fe/H] $\simeq -1.66$, red-HB (Dickens type 6), loose $c \simeq 1.0$, and relatively faint $M_V \simeq -5.5$ cluster (see [5]). A preliminary study of Palomar 3 has been published by Burbidge and Sandage [1]. They have found one variable star. Gratton and Ortolani [4] identified three RR Lyr stars and one possible Population II cepheid. They were not able to confirm the variability of the Burbidge-Sandage star. Later on 1999 Stetson et al [12] confirmed the variability status of Burbidge-Sandage and Gratton-Ortolani variable stars and suspected other 4 RR Lyr stars.

The limited number of variability studies for this cluster has ecouraged us to undertake a new survey of Palomar 3 to search for short-period variables. Special motivation for our study was provided by the noted possible presence of a Population II Cepheid in a red-HB cluster such as Palomar 3. As well known, Population II Cepheids are usually found in clusters with well-developed blue-HB tails only (see e. g. [10, 13]).

2. Observations and Data Reduction

Our analysis was based on approximately 50 CCD frames obtained during 6 nights: three in January 1997 at the 1.54 m telescope operated by the Steward Observatory, University of Arizona (1024×1024 pixels CCD, scale 0.38 arcsec/px), one night in February 1997 at the 2 m telescope of NAO "Rozhen", Bulgaria (375×242 pixels CCD, scale 0.32 arcsec/px), one in April 1999 at Steward Observatory and one in April, 2000 at NAO "Rozhen". The frames were obtained through V and I filters, and the exposure times for the frames varied between 6 and 15 minutes. The photometric reductions ware carried out using the DAOPHOT/ALLSTAR package [11] available in IRAF. Approximately 350 stars were identified on each frame and their instrumental magnitudes were determined. Following the method described in [3], we have selected one of the frames as a reference. The magnitudes determined for the other frames were converted by a first order least-squares fit to the reference frame system. The instrumental values were transformed to the standard (V, I) system by observing the standard field of M67 [2]. The errors from photometry and calibration are smaller than 0.07 for magnitude interval between 19 and 21 in V and I filters.

3. Search for Variable Stars

In our search for undetected variables we have used the following different methods.

3.1. Method of Kadla and Gerashchenko

The method proposed by Kadla and Gerashchenko [6] is based on the analysis of the color-magnitude diagram obtained from measurements of two images

taken within a time interval that is much shorter than the variability period. Thus the variables are at nearly identical phases and have to be located in the RR Lyr "gap". This method is suitable for the identification of RR Lyr candidates only. Applying this technique we confirmed the variability of the Burbidge and Sandage [1] candidate RR Lyr star (hereafter BS) and found five new suspected variables, all within 1 arcmin from the cluster center.

Table 1. Candidate variables: Kadla and Gerashchenko method

Name	X (arcsec)	Y (arcsec)	V	$V-I$	R (arcmin)
V1	−3.2	−2.3	20.27	0.75	0.06
V2	15.8	4.1	20.73	0.75	0.27
V3	−57.3	14.2	20.34	0.81	0.98
V4	25.7	18.6	20.61	0.78	0.53
V5	−60.7	35.0	20.62	0.87	1.17
BS	−28.4	−5.0	20.25	0.82	0.48

The candidate variables are given in (Table 1). In columns 2 and 3 of Table 1 the coordinates in arcsec of the new possible variables in the Sawyer-Hogg [9] system are listed. The next two columns give V and $V-I$ values, determined by only one image pair. R is the projected radial distance (in arcmin) from the cluster center.

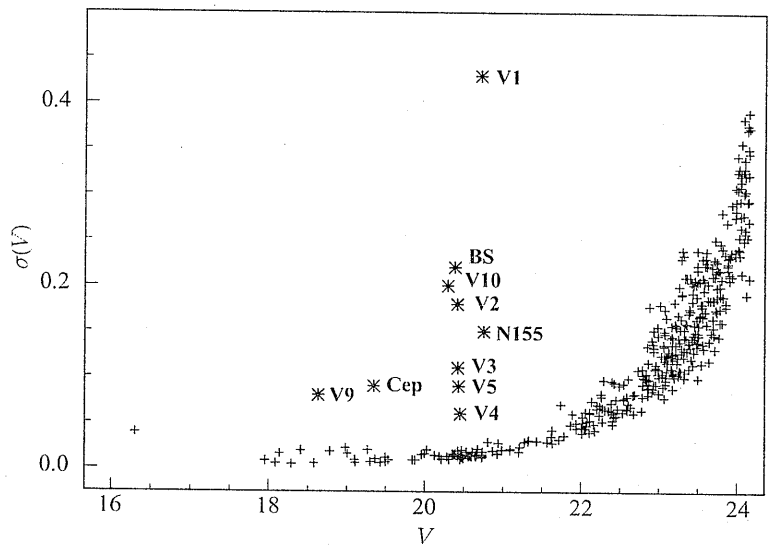

Fig. 1. Plot of the standard deviation vs. mean V magnitude
Possible variable stars are plotted as asterisks and the nonvariables as crosses

3.2. Comparison of the Brightness Variations

We determined the mean magnitudes and their standard deviations for the entire sample of stars. Naturally, the variables are expected to show much larger variations than the non-variable stars with the same brightness (Fig. 1). We found four additional candidates, including the Population II Cepheid, and the RR Lyr (No 155) suspected by Gratton and Ortonali [4]. The 4σ criterion would reject V4 and V5, found by the previous method. Table 2 lists the mean magnitudes and their variation for all the candidates, and for comparison, the typical observational uncertainties for the relevant magnitude interval. A plot of the standard deviation versus mean magnitude is shown in Fig. 1.

Table 2. Candidate variables: standard deviations of the magnitudes

Name	$\langle V \rangle$ "variables"	σ	$\langle V \rangle$ "normal stars"	σ
V1	20.71	0.43	20.5-21.0	0.03
V2	20.41	0.18	20.0-20.5	0.02
V3	20.42	0.11	20.0-20.5	0.02
V4	20.45	0.06	20.0-20.5	0.02
V5	20.43	0.09	20.0-20.5	0.02
BS	20.38	0.22	20.0-20.5	0.02
No 155	20.75	0.15	20.5-21.0	0.03
Pop. II Ceph.	19.34	0.09	19.0-19.5	0.01
V9	18.63	0.08	18.5-19.0	0.01
V10	20.29	0.20	20.0-20.5	0.03

3.3. Night-to-night Variations in the V Magnitude

As a further attempt to test the variability of the suspected stars we analyze night-to-night variations in the V magnitude. In Table 3 are given the mean magnitudes for the possible variables from three sets of observations. These stars present variations which are much larger than the variations of nonvariable stars of similar magnitude.

3.4. Variable Search Technique of Welch and Stetson

The availability of CCD observations in two filters separated by one month allowed us to apply the search technique of Welch and Stetson [14]. As described by these authors, "... the largest fraction of the flux change from a pulsating variable is due to the change in surface brightness-effective temperature, and hence the change in magnitude and color between any two epochs is correlated". *Nonvariable stars* have to be located near the origin in the diagram $V_1 - V_2$ versus $I_1 - I_2$ (where indices 1 and 2 indicate the values measured in

two different epochs), with dispersion equal to the errors of observations. The *variable stars*, on the other hand, have to be correlated in such a diagram.

Table 3. Candidate variables: night-to-night variations in V

Name	JD 244+		
	50466.59	50467.53	50490.54
V1	21.06	20.38	20.27
V2	20.22	20.62	20.73
V3	20.26	20.56	20.34
V4	20.45	20.44	20.61
V5	20.48	20.48	20.62
BS	20.25	20.66	20.25
No 155	20.82	20.71	20.62
Pop. II Ceph.	19.26	19.41	19.44
V9	18.63	18.70	18.72
V10	20.13	20.54	20.44

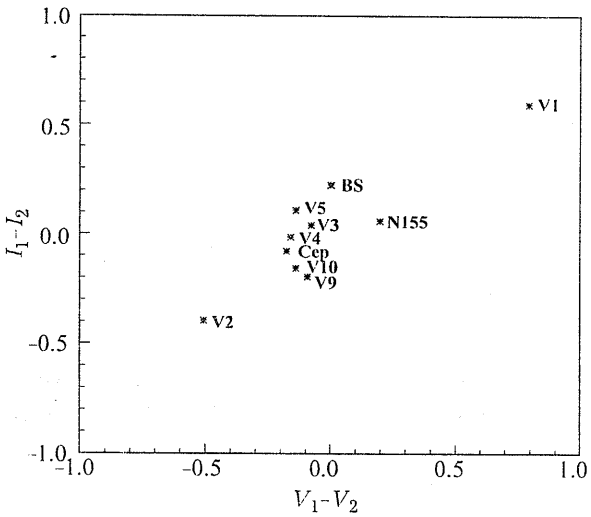

Fig. 2. The plot of $V_1 - V_2$ vs. $I_1 - I_2$
The indices 1 and 2 indicate the observations in January and February 1997, respectively

The magnitude differences $V_1 - V_2$ versus $I_1 - I_2$ for all possible variables of Palomar 3 are shown in Fig. 2. The indices 1 and 2 stand for the observations from January and February 1997, respectively. We have found that magnitude differences $V_1 - V_2$ and $I_1 - I_2$ of the candidate variables do seem to be correlated, although the correlation is not very strong. The locations of V3 and V4 are very close to $V_1 - V_2 = 0$ and $I_1 - I_2 = 0$, the region populated by nonvariable stars.

As a further attempt to test the variability of the stars we calculated the variability index I and variability ratio R of Welch and Stetson [14] for all stars in common between the two epochs. The variability index I is connected with changes in the brightness of the star in the two bandpasses and should be averaged zero for *nonvariable stars*. Each variable star will produce a variability index with a constant value, related to the amplitude of variation. Additional information of the nature of variation gives variability ratio R which is connected with temperature amplitude of the star.

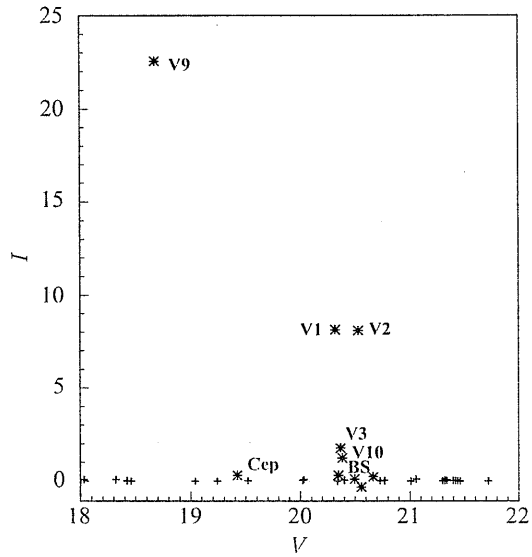

Fig. 3. A plot of the variability index I as a function of the average V magnitude The possible variable stars are plotted as asterisks and the nonvariables as crosses

Unfortunately, because of the small field of the CCD in our February 1997 run we have only 30 stars in common between two epochs. A plot of the variability index I as a function of the average V magnitude is shown in Fig. 3. The mean V magnitude, variability index I, variability ratio R and values of $I\sin(\arctan R)$, $I\cos(\arctan R)$ [14] for all suspected variable stars are given in Table 4. As can be seen, there are differences in the variability index and ratio of possible variables and nonvariable stars. The mean threshold of the nonvariable stars is $I = 0.2$ and $R = 0.1$.

Analysis of Table 4 shows that V1, V2, V9, V10, BS and the Population II Cepheid are as strong candidates, and leaves V4 and V5 bellow the 4σ statistical limit.

Table 4. Candidate variables: variability index I (Welch and Stetson)

Name	$\langle V \rangle$	I	R	$I\sin(\arctan R)$	$I\cos(\arctan R)$
V1	20.32	8.12	0.33	2.59	7.69
V2	20.54	8.08	1.60	6.85	4.28
V3	20.36	1.77	2.07	1.59	0.77
V4	20.49	0.12	23.68	0.12	0.00
V5	20.55	−0.31	1.21	−0.23	−0.19
BS	20.34	0.32	1.74	0.27	0.15
No 155	20.66	0.23	3.03	0.22	0.07
Pop. II Ceph.	19.42	0.31	2.14	0.28	0.13
V9	18.67	22.55	0.72	13.22	18.27
V10	20.38	1.23	1.13	0.92	0.82

According to Welch and Stetson [14] R ratio contains information about the contamination of stellar flux by fainter objects. They pointed that while a contamination by an object bluer than the variable would not change the R, a contamination by a redder one would increase the R. In our case there is no contamination of the Population II Cepheid by unresolved faint object. The variability ratio of most of the possible RR Lyr stars fall in the range from 1.13 to 2.07. The variable star V4 has a very large R value. We have no explanation for this result. The large R value for star No 155 can be explained with contamination by an unresolved companion.

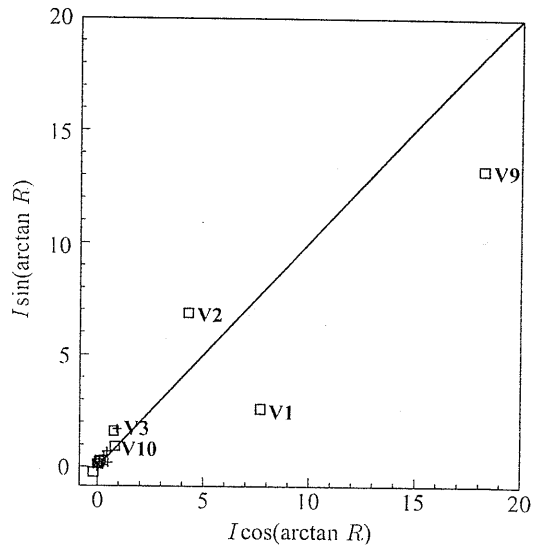

Fig. 4. A plot of $I\sin(\arctan R)$ vs. $I\cos(\arctan R)$ for all stars in common between the two epochs Possible variable stars are shown as squares

Figure 4 shows a plot of $I\sin(\arctan R)$ vs. $I\cos(\arctan R)$ which reveals probable variability and classification information directly. The nonvariable

stars are concentrated near the origin of the plot. The position of V9 in this diagram suggests that this star may be a red variable.

4. Light Curves

We searched the periods using a least-squares periodogram analysis by means of the phase dispersion minimization (PDM) task available in IRAF and a period-finding program based on Lafler and Kinman's [8] "theta" statistic. For the first time we have obtained the light curves and periods for 3 variable stars in Palomar 3: the Population II Cepheid has period $P = 3.402$ days, V1 and RR Lyr star No 155 from Gratton and Ortolani have periods $P = 0.567184$ and $P = 0.624152$, respectively. Unfortunately, the small number of CCD frames and very irregular time intervals did not permit us to obtain representative light curves and periods for the remaining suspected variables.

The V light curves are displayed in Figs 5 and 6.

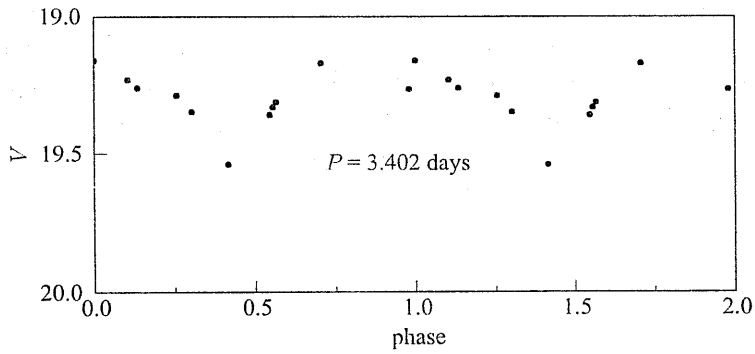

Fig. 5. The light curve of the Population II Cepheid

5. Summary

Using different techniques to search for variable stars in the globular cluster Palomar 3, we have reached the following conclusions:

- the RR Lyr star candidate from Burbidge and Sandage [1] was confirmed;
- we confirm the variability of the Population II Cepheid and determine the period $P = 3.402$ days;
- the RR Lyr star suspected by Gratton and Ortolani [4] has period $P = 0.624125$ days and is RRab Lyr type of star;
- the star V1 is also RRab Lyr type of star and has period $P = 0.567184$ days;
- V9 is probably a red variable;
- the status of V3, V5 and V10 remains uncertain.

The finding chart for the possible variables is shown in Fig. 7.

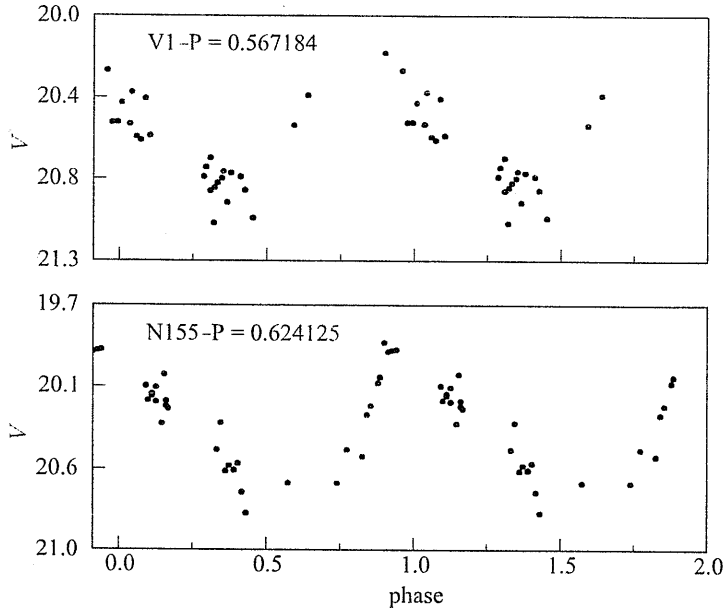

Fig. 6. The light curves of the V1 and No 155

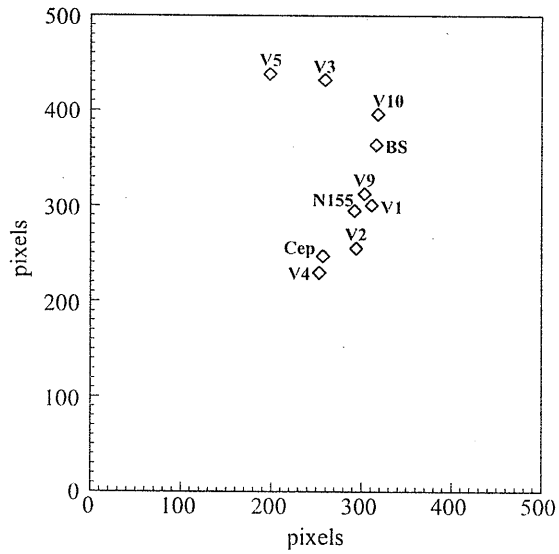

Fig. 7. Finding chart of the possible variable stars in the globular cluster Palomar 3 The size of the field is 3.98 arcmin. North is down and East is to the right

Acknowledgements

This research was supported in part by the Bulgarian National Science Fund grant under contract No F-812/1998 with the Bulgarian Ministry of Education and Sciences.

References

1. M. Burbidge and A. Sandage. ApJ **127** (1958) 527.
2. C. Christian, M. Adams, J. Barnes, D. Hayes, M. Siegel, H. Butcher and J. Mould. PASP **97** (1985) 363.
3. C. Clement and J. Bezaire. AJ **110** (1995) 5.
4. R. Gratton and S. Ortolani. A&AS **57** (1984) 177.
5. W. Harris. AJ 112 (1996) 1487.
6. Z. Kadla and A. Gerashchenko. Izv. Main A.O. of the Academy of USSR **199** (1982) 86.
7. S. Ortolani and R. Gratton. A&AS **79** (1989) 155.
8. J. Lafler and T. Kinman. ApJS **11** (1965) 216.
9. H. Sawyer-Hogg. Publ. David Dunlap Obs. **3** No 6 (1973).
10. H. Smith and A. Wehlau. ApJ **298** (1985) 572.
11. P. Stetson. *User's manual for DAOPHOT II* (1993).
12. Stetson et al. AJ **117** (1999) 247.
13. G. Wallerstein. ApJ **160** (1970) 345.
14. D. Welch and P. Stetson. AJ **105** (1993) 1813.